Digital image biological detection technology based on the porous silicon periodic crystals film*

YANG Jianfeng (杨建锋)[1], **JIA Zhenhong** (贾振红)[2,3]**, **LÜ Xiaoyi** (吕小毅)[2,3], **HUANG Xiaohui** (黄晓辉)[2,3], **and WANG Jiajia** (王佳佳)[2,3]

1. School of Physical Science and Technology, Xinjiang University, Urumqi 830046, China

2. School of Information Science and Engineering, Xinjiang University, Urumqi 830046, China

3. Key Laboratory of Signal Detection and Processing, Xinjiang Uygur Autonomous Region, Xinjiang University, Urumqi 830046, China

(Received 9 November 2020; Revised 25 December 2020)

In order to solve this problem, a new biological detection method is proposed, which makes use of the characteristics of optical transmission at the edge of the spectral band gap and sensitive to refractive index variation. When the probe light with wavelength at the edge of the Bragg band gap of porous silicon is incident on the surface of porous silicon, the change of refractive index caused by deoxyribonucleic acid (DNA) reaction in porous silicon will affect the detection light intensity transmitted from the porous silicon sensor. By analyzing the change of the average gray value of the transmitted light image, the concentration of the DNA can be obtained.

Document code: A **Article ID:** 1673-1905(2021)09-0552-6

DOI https://doi.org/10.1007/s11801-021-0176-5

Porous silicon is a kind of nano material with large specific surface area, good biocompatibility and adjustable refractive index[1,2]. Porous silicon optical biosensors can be prepared by electrochemical anodic corrosion and photolithography technology[3-5]. At present, there are two kinds of detection methods based on the change of fluorescence intensity and the change of refractive index[6-9]. Porous silicon optical biosensors based on fluorescence change usually use fluorescent markers to label biological probes, and detect target biomolecules by measuring the change of fluorescence intensity of reactants before and after biological reaction by fluorescence spectrometer. This kind of porous silicon sensor has periodic crystals film structure, which can enhance the fluorescence produced by the marker in porous silicon. The porous silicon biosensor based on fluorescence change has high detection sensitivity, but the fluorescent marker has certain influence on the detected biomolecules[10,11]. Porous silicon optical biosensors based on refractive index change usually use microcavity structure to detect the change of refractive index before and after biological reaction in porous silicon microcavity. There are two detection methods of refractive index. The first method is to measure the red-shift of the wavelength of spectrum defect state caused by the increase of refractive index of microcavity caused by biological reaction by reflection spectrometer[12]. The second method is to measure the change of defect reflected light intensity or transmitted light intensity with incident angle before and after biological reaction[13]. Although the sensitivity of porous silicon biosensor based on refractive index change is lower than that based on fluorescence change, it has the advantage of label free.

In order to improve the sensitivity and detection speed of refractive index detection method, Li Chuanxi et al[14] proposed to use 633 nm laser as detection light, incident porous silicon microcavity at different incident angles. The image on the surface of porous silicon microcavity is obtained by digital microscope, and the change of refractive index is measured by the change of gray level. Zhang Mi et al[15] proposed a detection method based on the change of gray value of porous silicon microcavity transmission image. In this method, the near infrared laser located at the low absorption band of porous silicon was incident on the surface of porous silicon microcavity before and after biological reaction. The infrared laser transmission was converted into visible fluorescence through up conversion card. The fluorescence image was received by digital microscope, and the average gray value of the image was calculated. The concentration of target molecules is measured by the change of the average gray value of the transmitted light image before and after biological reaction.

Due to the dispersion and absorption of the light transmitted in porous silicon, especially the visible light, and the random fluctuation of the interface, the optical characteristics of the defect state of the porous silicon microcavity devices prepared in the experiment are poor, and

* This work has been supported by the National Key R&D Program of China (No.2019YFC1606100), and by the National Natural Science Foundation of China (Nos.61665012, 61575168 and 11504313).

** E-mail: jzhh@xju.edu.cn

the actual measured reflection spectrum is far from the theoretical design value, resulting in the detection accuracy of biological detection affected[16]. In order to solve the problem of porous silicon microcavity, according to the good characteristics of the band gap edge of the reflection spectrum or transmission spectrum of the prepared porous silicon periodic crystals film is in good agreement with the theory, a biological detection is carried out by using the transmission characteristics of light wave which wavelength is located at the edge of spectral band gap is sensitive to the change of refractive index in this paper. A method of detecting the change of gray value of porous silicon image based on average periodic crystals film is proposed. A laser with a wavelength of 1 550 nm was used as the detection light of porous silicon biosensor. Near infrared band is the optical window of biomolecules. In addition, porous silicon periodic crystals film has small absorption of near infrared light, which can better play its optical properties[17,18]. A device with a central wavelength of 1680 nm has a thicker dielectric layer than that of a porous silicon device with a central wavelength in the visible light band. The detection error caused by the rough and uneven surface of porous silicon and the long wavelength of near infrared light is smaller than that of visible light[19]. In order to solve the problem that the digital microscope has no response to near infrared light, up-conversion card is used to convert near infrared light into visible fluorescence. The detection limit of porous silicon periodic crystals film biosensor can be further reduced by denoising the fluorescence image obtained by digital microscope. The proposed biological detection method has the advantages of low cost, fast speed, label free and high sensitivity.

The porous silicon periodic crystals film is a stack of alternating high and low refractive index layers, and its optical thickness satisfies the following relation:

$$n_H d_H = n_L d_L = \lambda_C/4, \quad (1)$$

where n_H and n_L are the refractive indices of the high and low refractive index layers, d_H and d_L are the optical thickness of the high and low refractive index layers, respectively. λ_C is the centre wavelength of the periodic crystals film. If the periodic crystals film reflector is set to 24 layers and the central wavelength is 1 680 nm, the high and low refractive indices are n_H=1.63 and n_L=1.32, respectively. According to Eq.(1), the thickness of each dielectric layer is calculated as 318.18 nm and 257.67 nm, the transmission spectrum before and after the deoxyribonucleic acid (DNA) reaction in the periodic crystals film is theoretically calculated by the transfer matrix method, and the excitation light (wavelength of 1 680 nm) is vertically incident to the surface of the periodic crystals film (θ=0°). The theoretical calculation results are shown in Fig.1, where curve a is the transmission spectrum diagram of the periodic crystals film before the DNA reaction (the high and low refractive indices are 1.32 and 1.63, respectively); b, c and d are the transmission spectrum diagrams after the high and low refractive indices of the periodic crystals film increase by 0.01 with the increase in composition of the biological reaction.

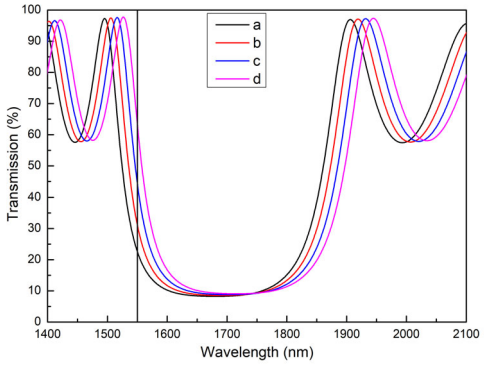

Fig.1 Theoretical calculation of the transmission spectra of the periodic crystals film before and after the DNA reaction

Fig.1 shows that the effective refractive index of the device increases with the increase in target molecular concentration of the DNA reaction in the periodic crystals film. The transmission spectrum of the device is red-shifted, and the light transmittance increases at the forbidden edge (wavelength of 1 550 nm). The relationship between transmittance variation (ΔI) and refractive index variation (Δn) is shown in Fig.2. When the change in refractive index is greater than 0.05, the transmittance tends to be saturated.

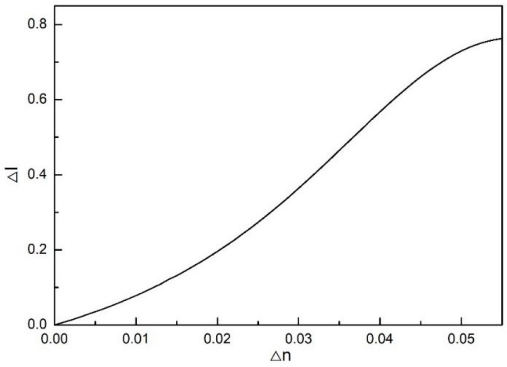

Fig.2 Variance of the transmittance with the refractive index of the device

By analyzing the relationship between the change of the transmittance at the edge of the band gap and the effective refractive index of the device after the DNA reaction, the change of the transmittance (ΔI) can be indicated by the change of the average gray value (ΔG) of the transmitted light image of the periodic crystals film. The digital microscope receives the image of transmitted light and calculates the average grey value of the image. The change in transmission light intensity will lead to the change in grey value of the transmission light image.

Therefore, we can quantitatively detect the concentration of target molecules of the DNA reaction in the periodic crystals film based on the change in average grey value.

The porous silicon samples must be oxidized and functionalized, and the DNA must be immobilized before the sensor is made. The refractive index of the device decreases and the reflection spectrum both blue shift after oxidation treatment. Functionalization and fixation of DNA will increase the refractive index and red shift the reflectance spectrum. The blue shift and red shift of the device will cause the edge position of the transmission spectrum to deviate from the wavelength of the monitoring light. To solve this problem, we can change the incident angle of the excitation light. Fig.3(a) shows the transmission spectrum at different incident angles calculated by the transfer matrix method theory. In Fig.3(a), the increase in incident angle causes the blue-shift of the reflection spectrum of the device. Fig.3(b) shows the relationship between the blue-shift of the reflection spectrum and the incident angle. The analysis shows that the blue-shift of the transmission spectrum increases with the increase in incident angle. Therefore, by adjusting the angle of incidence, the transmission spectrum edge of the sample can be partially shifted to the original design position.

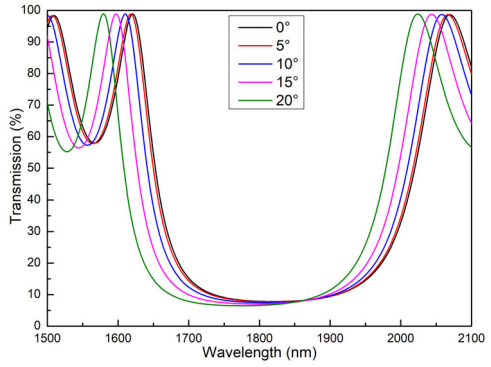

(a)

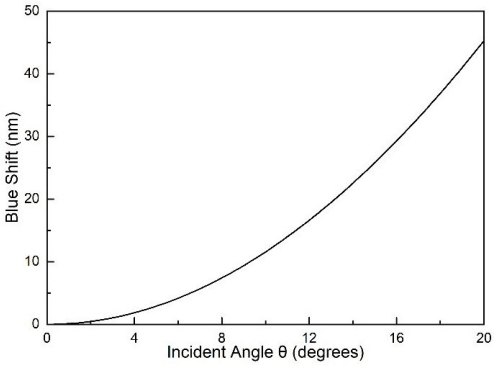

(b)

Fig.3 (a) Transmission spectra at different incident angles; (b) Relationship between blue shift and incident angle of the transmission spectrum

P-type monocrystalline silicon (boron-doped amorphous silicon <100> with a resistivity of 0.01 — 0.03 Ω·cm, 400±10 μm) was produced as a periodic crystals film. Before the experiment, the P-type single crystal silicon was cut into a small square with an area of 2 cm×2 cm and cleaned with anhydrous ethanol and deionized water in an ultrasonic cleaning machine for 20 min to remove oil impurities on the surface of the silicon wafer. The 40% hydrofluoric acid solution and 99% anhydrous ethanol were uniformly configured into a corrosion solution at 1:1 volume ratio. We placed the cleaned silicon wafer at the bottom of the corrosion tank (the corrosion tank was made of polytetrafluoroethylene) and poured the corrosion liquid into the corrosion tank for approximately 6 mL. The current densities of the high and low refractive index layers were set to 110 mA/cm^2 and 40 mA/cm^2, respectively, by the Labview program; the corrosion time was 2.5 s and 3 s, respectively. After a layer of porous silicon medium was formed, the interval was 3 s to supplement sufficient fluoride and ensure a uniform corrosion of porous silicon. After the corrosion finished, the silicon wafer was repeatedly washed with anhydrous ethanol and deionized water to remove the residual corrosion solution on its surface and dried in nitrogen. A porous silicon periodic crystals film reflector with a central wavelength of 1 680 nm was prepared under these conditions. The transmission spectrum of the periodic crystals film, which was detected by a spectrometer with a resolution of 0.1 nm (Hitachi U-4100, purchased from Japan Hitachi Company), was compared with the theoretical calculated transmission spectrum as shown in Fig.4.

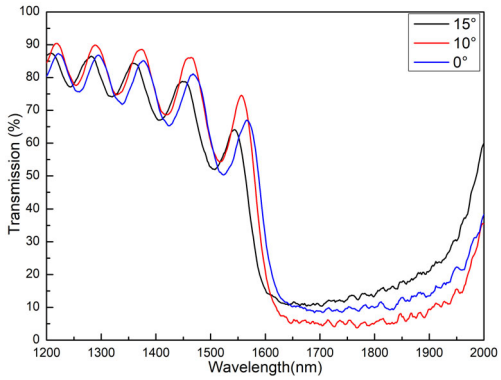

Fig.4 Comparison between experimental transmission spectrum and theoretical calculation of the periodic crystals film reflector

According to Fig.4, there are differences between experimental and theoretical calculations of the transmission spectra, since the dispersion, absorption and fluctuation of the porous silicon interface are not considered in the calculation process. The dispersion will narrow the band gap of the periodic crystals film, and the absorption and fluctuation of the interface will reduce its bandgap reflectivity.

A newly prepared periodic crystals film surface morphology and its cross section diagram are observed by

scanning electron microscopy, as shown in Fig.5. Fig.5(a) shows that its pore size is 20—30 nm, the DNA are fully accessible, and the biological reactions and biological detection occur. The composition of each layer in Fig.5(b) is porous silicon.

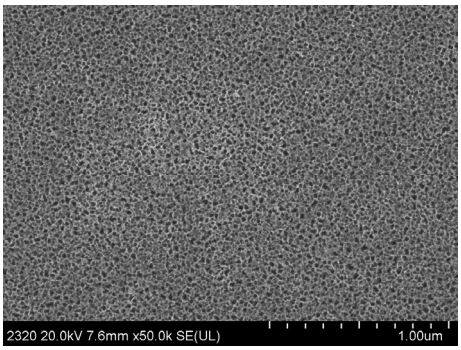

(a)

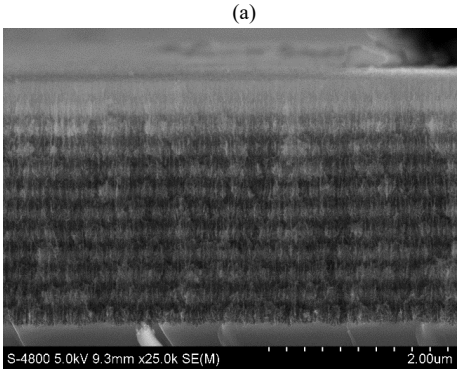

(b)

Fig.5 (a) Surface morphology of the periodic crystals film; (b) Cross section of the periodic crystals film

There are many Si-H bonds on the surface of the dried periodic crystals film sample, which result in its unstable properties, are easily oxidized in air and must be oxidized. To couple the DNA to the periodic crystals film holes, it is also necessary to conduct the silanization and glutaraldehyde treatment, so that the surface-modified amino and aldehyde groups react with hydroxyl and carboxyl groups in the DNA, respectively, to achieve DNA immobilization.

Oxidation treatment: Soak the dried periodic crystals film sample in 40% H_2O_2 solution and place it in a vacuum drying oven at 60 ℃. After 3 h of reaction, oxidize the Si-H bond on its surface to form the Si-O bond. Remove the sample and repeatedly wash it with deionized water and anhydrous ethanol. Dry the sample in nitrogen.

Silanization treatment: Immerse the oxidized sample in the 5% concentration of APTES solution (which is composed of aminopropyltriethoxysilane, methanol and deionized water with a volume ratio of 1:10:10). Remove the sample after approximately 1 h. Repeatedly wash the remaining ATPES solution on the sample surface with deionized water and dry the sample at room temperature. Then, place the sample in a vacuum drying oven at 100 ℃ for 10 min.

Glutaraldehyde treatment: Immerse the silanized sample into an aqueous solution of 2.5% glutaraldehyde (prepared from glutaraldehyde and deionized water at a volume ratio of 1:19). After 1 h reaction, remove and repeatedly wash the sample with PBS (pH=7.4) to remove the residual glutaraldehyde solution on the surface, dry the sample at room temperature.

Each stage of the periodic crystals film functionalization must be examined by a spectrometer to verify the successful silanization of porous silicon. Fig.6 shows the spectral contrast diagram of the periodic crystals film at different stages of functionalization. The central wavelength of the sample is blue-shifted after oxidation, since the Si-O bond has a smaller refractive index than the Si-H bond. After the silanization and glutaraldehyde treatment, amino groups and aldehyde groups were modified in the pores of the samples, which increased the effective refractive index of porous silicon and red-shifted the central wavelength of the porous silicon spectrum.

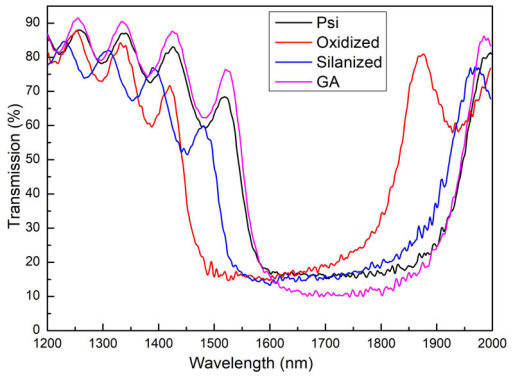

Fig.6 Spectral comparison of periodic crystals film at different stages of functionalization

First, 40 μL probe DNA (5′-CAACGTTGCAGTGTAC-3′-NH2) with 16 base pairs was dropped onto the surface of the functionalized periodic crystals film reflector s-ample using a micropipette. We put the sample in a thermostat with a temperature of 37 ℃, removed it after 2 h, repeatedly washed the sample surface with phosphate buffer and deionized water to remove the probe DNA that was not modified on the porous silicon periodic crystals film, and dried it in air. Then, the dried sample was immersed into a solution of 3 M ethanolamine hydrochloride and placed in a 37 ℃ thermostat for approximately 1 h. To seal the unreacted aldehyde group, the sample surface was repeatedly rinsed with phosphate buffer and deionized water and dried in air. Finally, 40 μL target DNA (3'-GTTGCAACGTCACATG-5') with 16 base pairs was added to the sample surface that contained the probe DNA using a micropipette and placed in a thermostat at 37 ℃ for approximately 2 h. After removal, it was rinsed with PBS and deionized water to remove the unreacted target DNA.

Fig.7 is a schematic diagram of the detection device of the biosensor. The detection light is generated by a semiconductor laser (λ=1 550 nm, 100 MW); The probe light is transformed into parallel beam by collimating beam expander L_1 and L_2; A part of parallel beam is reflected to the detector by beam splitter to monitor whether the laser power is stable; The porous silicon sample is placed in the center of the goniometer with a resolution of 1′. The incident angle of the probe light can be adjusted by rotating the goniometer; The parallel beam of porous silicon sample reaches the upconversion card to form visible fluorescence. The fluorescence image on the upconversion card is obtained by digital microscope and displayed by computer.

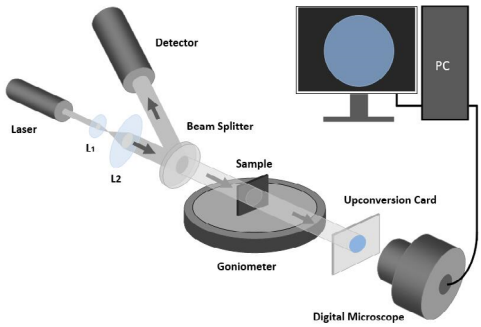

Fig.7 Schematic diagram of the detection path

In the process of receiving the transmitted light image of periodic crystals film, the digital microscope will be disturbed by noise, which will affect the calculation accuracy of image gray value. The median filtering algorithm can be used to denoise the image. The image after noise removal and the original image are shown in Fig.8. The green circular area with a radius of 150 pixels centered on the center of porous silicon is selected in the image by Matlab software, and the average gray value of the circular area is calculated.

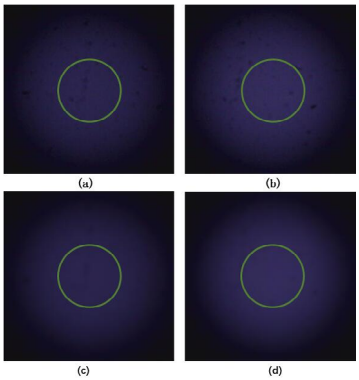

Fig.8 Original images (a) before and (b) after adding DNA; Images after noise removal (c) before and (d) after adding DNA

The selected DNA concentrations are 1 nM, 2 nM, 5 nM, 10 nM, 50 nM and 100 nM, respectively. The gray value of the transmitted light image after noise removal is calculated. The variation trend of the concentration of DNA and the average gray value is shown in Fig.9.

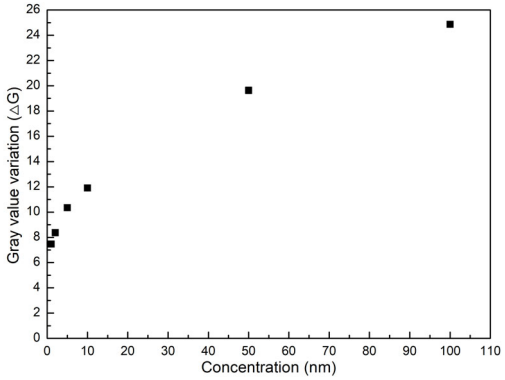

Fig.9 Trend of concentration and gray value variation after noise removal

With the increase of target DNA concentration, the change of average gray value will also increase. At the concentrations of 1 nM, 2 nM, 5 nM and 10 nM, there is a good power exponential relationship between the average gray value and the target molecular concentration. The fitting result is shown in Fig.10, and the fitting equation is

$$Y=6.524+0.996X-0.046X^2. \quad (2)$$

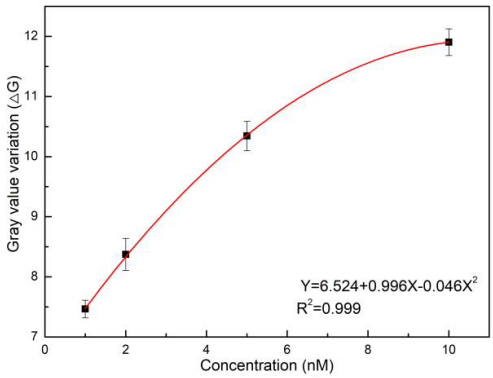

Fig.10 The fitting relationship between the concentration and the change of gray value

$$\sigma=\sqrt{\frac{\sum_{i=1}^{n}(X_i-\bar{X})^2}{n-1}}, \quad (3)$$

where σ is the standard deviation of the average grey value of the same sample before the biological reaction for 10 consecutive measurements, n is the number of measurements, and X is the average grey value of the sample before the biological reaction. According to the experimental σ=0.31, for the samples in Fig.10, if the image is not denoised, the experimental σ=0.35. The experimental results show that the variance of gray value variation can be reduced and the detection accuracy can be improved by denoising the transmitted light image.

According to Eq.(2), It is assumed that the concentration of DNA molecule is 0 , the change of the gray value

variation of the sample is greater than 3σ, so 3σ rule can not be used to determine the detection limit in our experiment. Obviously, the detection limit of our method is less than 1 nM.

The sensitivity of this method is better than that of the image detection method based on porous silicon microcavity. The detection limit of the proposed detection method for DNA is lower than the 4 nM detection limit of the method based on the defect state of porous silicon microcavity[15]. In addition, the fabrication of porous silicon periodic crystals film structure is easier than that of porous silicon microcavity structure.

In this paper, a new biosensor detection method is proposed, which makes full use of the advantage that the wavelength is located at the edge of the band gap of one-dimensional photonic crystal and is sensitive to the change of refractive index. By design and preparation, the band gap edge of porous silicon periodic crystals film device is located near 1 550 nm. The infrared laser at 1 550 nm is used as probe light, and the transmitted light is converted into visible fluorescence by upconversion card. The visible fluorescence image is obtained by digital microscope. The DNA reaction in the porous silicon periodic crystals film sensor increases the equivalent refractive index of the device, which changes the detection light intensity of the sensor and changes the average gray value of the fluorescence image. The concentration of target DNA can be detected by measuring the average gray value of fluorescence image before and after DNA reaction. The experimental results show that the variance of gray value can be reduced by denoising the fluorescence image. The detection limit of the proposed detection method for DNA which is better than 4 nM detection limit of the method based on the defect state of porous silicon microcavity. Our detection method has the advantages of low cost, fast and high sensitivity.

References

[1] G. Palestino, V. Agarwal, R. Aulombard, E. Pérez and C. Gergely, Langmuir **24**, 13765 (2008).

[2] A. H. Soeriyadi, B. Gupta, P. J. Reece and J. J. Gooding, , Polymer Chemistry **5**, 2333 (2014).

[3] S. D. Campbell, Journal of Vacuum Science & Technology B: Microelectronics and Nanometer Structures Processing, Measurement, and Phenomena **13**, 1184 (1995).

[4] M. I. N. M. Isa, J. E. Tham, K. S. Chan, Malaysian Journal of Analytical Ences **15**, 227 (2011).

[5] W. R. Zhao, J. D. Chen, J. Ding and S. J. Chen, Journal of Shantou University (Natural Science Edition) **21**, 43 (2006). (in Chinese)

[6] I. A. Levitsky, W. B. Euler, N.Tokranova and A. Rose, Applied Physics Letters **90**, 1781 (2007).

[7] F. S. H. Krismastuti, S. Pace and N. H. Voelcker, Advanced Functional Materials **24**, 3639 (2014).

[8] D. B. Dimitrov, I. Savatinova and E. Liarokapis, Opto-Electronics Review **1998**, 295 (1998).

[9] D. R. Huanca, D. S. Raimundo and W. J. Salcedo, Microelectronics Journal **40**, 744 (2009).

[10] Y. Li, Z. Jia, G. Lv, H. Wen, P. Li, H. Zhang and J. Wang, Biomedical Optics Express **8**, 3458 (2017).

[11] Z. Guo, Z. Jia, J. Yang, K. Nikola and C. Li, Sensors **17**, 1335 (2017).

[12] H. Zhang, Z. Jia, X. Lv, J. Zhou and J. Ma, Biosensors & Bioelectronics **44**, 89 (2013).

[13] P. Li, Z. Jia and G. Lü, Scientific Reports **7**, 44798 (2017).

[14] C. Li, Z. Jia, P. Li, H. Wen, G. Lv and X. Huang, Sensors **17**, 750 (2017).

[15] M. Zhang, Z. Jia, X. Lv and X. Huang, IEEE Sensors Journal **20**, 12184 (2020).

[16] T. Okazaki, T. Imasaka and N. Ishibashi, Analytica Chimica Acta **209**, 327 (1988).

[17] M del M. Fernández-Carrobles, G. Bueno, O. Deniz, J. Salido and M. Garcia-Rojo, IEEE Journal of Biomedical & Health Informatic **18**, 999 (2014).

[18] J. Sun, Microwave & Optical Technology Letters **33**, 240 (2002).

[19] C. I. Li, Z. Jia, L. He and X. H. Huang, Optoelectronics Letters **15**, 89 (2019).